Determination of the Central Axis of the Scaphoid

Dennis J. Heaton, MS[1] Thomas Trumble, MD[2] Diana Rhodes, DVM, PhD[3]

[1] Pacific Northwest University of Health Sciences, College of Osteopathic Medicine, Seattle, Washington
[2] Bellevue Bone and Joint Physicians, Bellevue, Washington
[3] Pacific Northwest University of Health Sciences, Yakima, Washington

Address for correspondence Dennis J. Heaton, MS, 915 Harvard Ave., Billings, MT 59102 (e-mail: djheato@yahoo.com).

J Wrist Surg 2015;4:214–220.

Abstract

Purpose Determine the central axis of the scaphoid and its relation to surrounding anatomic landmarks to facilitate internal fixation of the scaphoid.

Methods Seventeen cadaveric dissections of the wrist were performed. Measurements of the height and width of the proximal pole, waist, and distal pole were made. The midpoint of the height and width of each measurement were plotted on a scatter plot graph and a forecast line was developed. The formula of the resultant line was used to calculate the position of the central axis at the proximal pole, waist, and distal pole. The inverse tangent of the slope of the line was then used to determine the angle of the line from proximal to distal.

Results The average central axis fell along a line measuring at points from the ulnar to the radial border and from the dorsal to the volar border of the proximal pole, waist, and distal pole at 7.86 mm, 7.61 mm, and 7.31 mm respectively; an angle of 13.78 degrees from ulnar to radial and dorsal to volar. The proximal point can be determined by measuring ~44 mm radially from the ulnar styloid along the watershed line of the radius and 14 mm volar from the dorsal tip of the Lister tubercle. The distal point can be determined by measuring ~4 mm ulnar from a line extending distally from the volar radial corner, and 7 mm volar from the most dorsal point of the combined surface of the trapezium and triquetrum. No significant difference existed between male and female specimens.

Conclusions The central axis of the scaphoid can be described to exist along a line extending from the relative central point of the proximal pole, measured 7.86 mm radial from the scapholunate ligament and 8.31 mm volar of the most dorsal point; through the waist, and extending to the relative central point of the distal pole measured 3.77 mm ulnar of the volar radial corner and 7.36 mm volar of the most dorsal point at an angle directed radially and volarly at 13.78 degrees.

Level of Evidence Level III

Type of Study Diagnostic/ therapeutic.

Keywords

- scaphoid axis
- scaphoid anatomy
- scaphoid targeting
- volar scaphoid approach

Scaphoid fractures account for approximately 70% of carpal bone fractures.[1–8] Because of the unusually tenuous vascular supply to the scaphoid, as well as the majority of its substance being composed of articular cartilage, nonunion and malunion are common complications, most often associated with proximal pole fractures.[1–8] Treatment providing the greatest stability of the fracture is most desirable to limit the risk of nonunion. Several biomechanical studies have been

DOI http://dx.doi.org/10.1055/s-0035-1556857.
ISSN 2163-3916.

performed to address this problem. Because of the favorable results of internal fixation, minimally displaced and acutely displaced scaphoid fractures are often treated with intraosseous screw fixation.[2,4–6,8]

In addition to the scaphoid's unusual vascular pattern, it has a very unusual shape. Several studies have described the surface pattern of the scaphoid, its mean length, and differences in morphometric data between sexes, as well as the kinematics of the carpals. These studies have helped to clarify the mechanism of injuries as well as assisting in the improvement of surgical technique and injury prognosis. However, a paucity of literature has been published to describe the central axis of the scaphoid, the target for internal screw fixation.[2–5]

The purpose of this study is to describe the mean position of the central axis of the scaphoid and how to identify it utilizing practical surgical landmarks. This description would enable more confident screw placement during surgical treatment of scaphoid fractures.

Materials and Methods

Seventeen cadaveric specimens were dissected for this study. Guidelines set forth by the author's institution were followed for the use of each cadaver for research to be performed. Additional permission was attained for cadavers that originated from an outside institution. Specimens were excluded if there was evidence of a previous injury, Eaton stage IV osteoarthritis, or any other condition resulting in severe deformity of the scaphoid. All measurements were performed on the right upper extremity. The right upper extremity was used because of its propensity as the dominant extremity and to maintain reproducibility. There was no documentation available to ascertain true dominant laterality. Measurements, excluding intra-articular measurements, were performed twice and on separate dates. A Kobalt handheld digital caliper, model number 53247 (Lowe's Manufacturing, Mooresville, NC, USA) was used to make the required measurements. Measurements were documented to the nearest hundredth of a millimeter. The caliper was zeroed prior to each measurement.

Cadavers examined for the study had their sex documented for comparative analysis. Age was not included in the demographics.

A dorsal and volar approach was required to adequately expose the scaphoid and the radioscaphoid, scaphocapitate, scapholunate, and scaphotrapeziotrapezoidal joints. The wrist capsule was sharply dissected extending from the third metacarpal to the volar surface of the first carpometacarpal, and then dissected proximally. Care was taken not to destabilize the scaphoid in its intra-articular position.

Once adequate exposure of the scaphoid was attained, intra-articular measurements were performed. The long axis of the scaphoid was measured from the most proximal articular surface to the most distal articular surface of the distal pole. The dorsoradial ridge was used as the anatomic landmark separating the proximal from the distal articular surface.[1] The proximal pole dorsal-volar distance was measured from the proximal tubercle to its most volar point; the radioulnar distance was measured from the radial edge of the

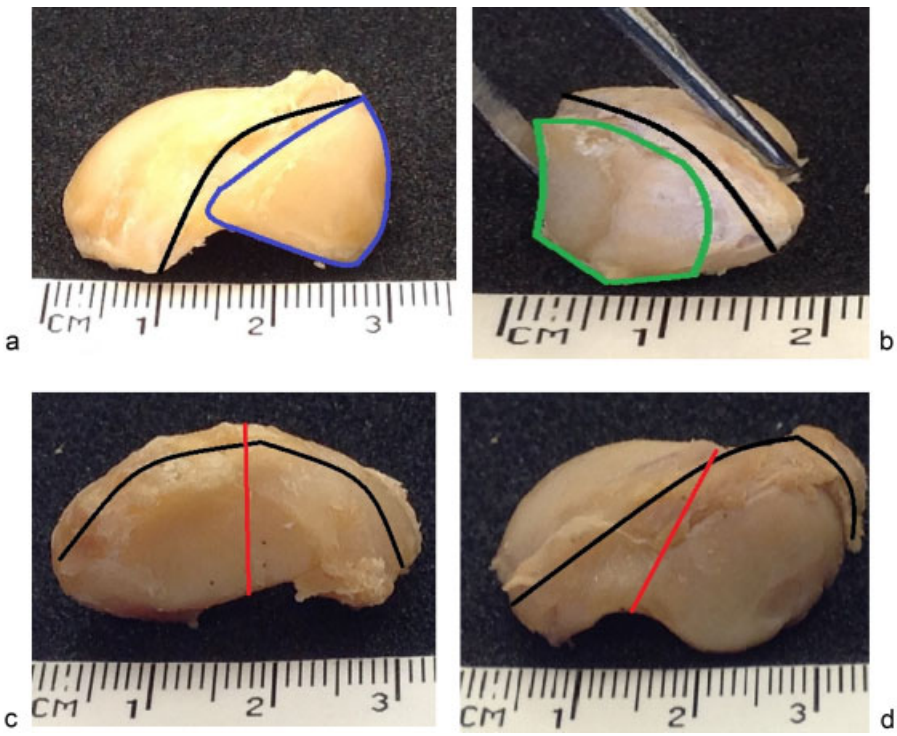

Fig. 1 Relative position of the three anatomic landmarks used to make measurements to further elucidate the central axis; the black line representing the general position of the dorso-radial ridge as viewed from various positions of the scaphoid. **(a)** The proximal pole is outlined in blue. **(b)** The distal pole is outlined in green. **(c)** The height of the waist is outlined in red. **(d)** The width of the waist is outlined in red.

dorsoradial ridge to the scapholunate joint (►**Fig. 1a**). The distal pole dorsal-volar distance was measured from its most dorsal point to its most volar point (►**Fig. 1b**). The radioulnar distance of the distal pole was measured using the most ulnar point on the scaphotrapezoid joint to the radial edge on the distal dorsoradial ridge (►**Fig. 1b**). The waist dorsal-volar distance was measured at the most narrow point of the scaphocapitate joint extending from dorsal to volar (►**Fig. 1c**). The radioulnar distance of the waist was also measured at the most narrow point of the scaphocapitate joint extending from the ulnar to radial surface (►**Fig. 1d**).

A carpectomy was performed following the intra-articular measurements. Remaining soft tissue was sharply dissected off of the scaphoid, with care not to disrupt the surface features. Extra-articular measurements included the long axis and the dorsal-volar and radioulnar distances of the proximal pole, of the waist, and of the distal pole. The same surface landmarks used to make the intra-articular measurements were used for the extra-articular measurements.

The dorsal-volar and radioulnar distances of the articular surfaces of the radius, lunate, capitate, and the combined trapezium and triquetrum were acquired following the extra-articular measurements of the scaphoid. The dorsal-volar distance of the radius extending from the Lister tubercle to the volar watershed line was documented, as well as the radioulnar distance of the radioulnar joint from the ulnar styloid process to the radial styloid process. These measurements were acquired to provide clinically identifiable landmarks and their association to the central axis, thus enabling more accurate identification of the proximal and distal points of the axis in a clinical setting.

All of the measurements were documented with the appropriate identifier for each specimen, and secondary measurements were confirmed to belong to the same specimen.

The mean for each primary and secondary measurement was calculated for each specimen, and the overall mean was calculated for all data points across the entire study population.

The mean central point for the proximal pole, waist, and distal pole was calculated at the intersection of the line extending from the midpoint of the dorsal-volar and radioulnar distances. The mean central points for the proximal pole, waist, and distal pole were plotted along a scatter plot graph. Linear regression analysis was used to calculate the trend line through the center of the points. The formula of the line was then used to calculate the point for each region that lay on the central line. The inverse tangent of the slope of the line was used to determine the angle of the central line.

Results

Seventeen specimens (six female and eleven male) were analyzed for the study. The overall mean for each measurement and sex-specific data are displayed in ►**Table 1**. An unpaired *t*-test was used to compare the intra-articular to

Table 1 Averages for intra- and extra-articular measurements

Scaphoid measurement	Mean (SD)	Female (SD)	Male (SD)
Intra-articular measurements			
Long axis	28.631 (±2.928)	27.887 (±2.616)	29.078 (±3.145)
Proximal pole height	15.408 (±2.758)	13.255 (±2.440)	16.699 (±2.105)
Proximal pole width	16.594 (±3.145)	16.185 (±3.370)	16.839 (±3.162)
Waist height	13.597 (±1.806)	12.058 (±1.316)	14.367 (±1.527)
Waist width	11.391 (±1.610)	11.086 (±1.367)	11.543 (±1.768)
Distal pole height	16.369 (±1.989)	14.756 (±1.165)	17.175 (±1.840)
Distal pole width	14.444 (±2.209)	13.242 (±2.081)	15.112 (±2.089)
Extra-articular measurements			
Long axis	28.359 (±2.039)	26.812 (±1.134)	29.760 (±1.612)
Proximal pole height	16.619 (±1.641)	15.049 (±0.724)	17.559 (±1.255)
Proximal pole width	16.851 (±2.138)	16.312 (±2.220)	18.135 (±1.869)
Waist height	13.328 (±1.801)	11.893 (±1.714)	14.307 (±1.159)
Waist width	11.048 (±1.042)	10.280 (±1.175)	11.617 (±0.546)
Distal height	13.521 (±1.964)	12.912 (±1.917)	14.332 (±1.883)
Distal width	14.066 (±1.686)	13.595 (±1.304)	15.820 (±1.314)

Intra-articular and postcarpectomy average measurements with standard deviation are displayed. The first column represents the overall averages across sexes.
Female and male specific measurements are displayed in columns 2 and 3, respectively.
No significant difference existed between intra-articular and extra-articular measurements ($p = 0.997$) or between sexes ($p = 0.399$).

Table 2 Average articular measurements

Articular surfaces	Average (SD)
Radial height	14.238 (±1.347)
Radial width	14.165 (±1.848)
Lunate height	15.215 (±1.766)
Lunate width	6.988 (±1.793)
Capitate height	13.610 (±1.365)
Capitate width	13.223 (±1.156)
Trapezium and triquetrum height	13.141 (±2.276)
Trapezium and triquetrum width	16.527 (±4.259)
Radioulnar measurements	**Average (SD)**
Radial height	26.815 (±2.480)
Radioulnar width	52.508 (±2.939)

Average measurements of the height and width of the articular surfaces of the radius and surrounding carpal bones, with standard deviations. This includes the overall height of the radius and the radioulnar joint width. The measurements of the articular surfaces are important in further defining the central axis and its relationship to surrounding structures.

extra-articular measurements. A *p*-value of 0.997 was calculated; thus there was no significant difference between intra-articular and extra-articular measurements. Analysis of the extra-articular measurements showed the mean dorsal-volar and radioulnar distances of the proximal pole to measure 16.62 (±1.64) and 16.85 (±2.14) millimeters, the waist to measure 13.33 (±1.80) and 11.05 (±1.04) millimeters, the distal pole to measure 13.52 (±1.96) and 14.07 (±1.69) millimeters, and the long axis to measure 28.36 (±2.04) millimeters.

The radioulnar and dorsal-volar distances of the articular surfaces of the radius, lunate, capitate, and combined

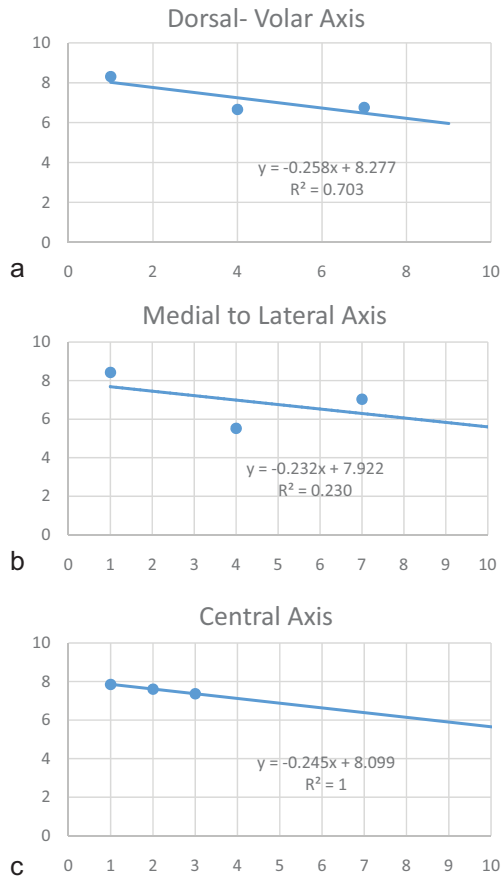

Fig. 2 Scatter plot graphs representing the line of the axes and the overall central axis. The *y*-axis represents a measurement in mm, the *x*-axis represents position from proximal to distal, with lower numbers on the x-axis representing a proximal position and higher numbers representing a more distal position. **(a)** Line of the dorsal-to-volar axis. **(b)** Medial-to-lateral axis. **(c)** Overall central axis. The equation for the line and the regression analysis value are displayed in each respective plot.

Table 3 Central axis points and angle

Overall	Dorsal-volar axis	Medial-to-lateral axis	Central axis
Angle	14.477 degrees	13.067	13.777
Proximal pole	8.019	7.690	7.855
Waist	7.245	6.994	7.610
Distal pole	6.468	6.298	7.364
Male	**Dorsal-volar axis**	**Medial-to-lateral axis**	**Central axis**
Angle	38.893	30.058	34.710
Proximal pole	8.779	9.068	8.220
Waist	7.153	5.085	7.527
Distal pole	7.166	7.910	6.834
Female	**Dorsal-volar axis**	**Medial-to-lateral axis**	**Central axis**
Angle	28.120	34.231	31.274
Proximal pole	7.525	8.158	7.278
Waist	5.946	5.140	6.670
Distal pole	6.456	6.798	6.063

The dorsal-to-volar axis, medial-to-lateral axis, and final central axis calculations, including the angle, derived from the formula of the lines that are displayed in ►**Fig. 3** and ►**Fig. 5**.

trapezium and triquetrum, as well as the radioulnar joint, are displayed in ►**Table 2**.

The mean central point for the study population, calculated by dividing the mean of each radioulnar and dorsal-volar distance of each respective landmark by 2, for the dorsal-volar axis of the proximal pole, waist, and distal pole measured 8.31, 6.66, and 6.76 mm respectively. A linear regression analysis ($R^2 = 0.703$) was used to plot a forecast line extending through the central points of the dorsal-volar axis, with the formula $y = -0.2582x + 8.2773$. Using this formula, the points along the dorsal-volar axis were calculated and equaled 8.02, 7.25, and 6.47 mm for the proximal pole, waist, and distal pole, respectively (►**Table 3**). The angle of the axis, determined by the inverse tangent of the slope of the line, measured 14.48 degrees directed volar from a line running parallel to the dorsal surface of the scaphoid.

The mean central point for the study population for the radioulnar axis, calculated using the same formula described above, of the proximal pole, waist, and distal pole measured 8.43, 5.52, and 7.03 mm respectively. A linear regression analysis ($R^2 = 0.230$), was used to plot a forecast line extending through the central points of the radioulnar axis, with the formula $y = -0.2321x + 7.9225$. Using this formula, the points of the radioulnar axis were calculated and equaled 7.69, 6.99, and 6.30 mm for the proximal pole, waist, and distal pole respectively (►**Table 3**). The angle of the axis, determined by the inverse tangent of the slope of the line, measured 13.07 degrees directed radial from a line running parallel to the ulnar surface of the scaphoid.

The central axis was calculated using the mean calculations of the lines for the dorsal-volar and radioulnar axes. The formula for the line of the central axis equaled $y = -0.2452x + 8.0999$. Therefore the mean central axis of the scaphoid was calculated to exist at 7.86, 7.61, and 7.36 mm volar and radial at the proximal pole, waist, and distal pole respectively. Linear regression analysis measured $R^2 = 1$, confirming these points correlated directly to the calculated central axis. The angle of the axis was determined by the inverse tangent of the slope of the line; this measured 13.78 degrees from the proximal pole point directed in a volar-radial direction (►**Table 3**) (►**Figs. 2a–c**, **3a, b**).

The proximal point of the axis can be identified by articular landmarks to exist 13.56 mm volar from the most dorsal point of the Lister tubercle and 43.77 mm radial from the ulnar styloid process, 7.86 mm radial from the scapholunate ligament, and 8.74 mm ulnar from the radial styloid. The distal point of the axis can be identified to exist 7.17 mm volar from the most dorsal point of the combined trapezium and triquetrum and 3.77 mm ulnar from the volar radial corner (►**Fig. 4a–c**).

Male and female specimens were analyzed separately. The central axis for the male specimens was calculated to exist along a line with the formula $y = -0.6927x + 8.9123$, $R^2 = 1$, at points calculated in a volar radial direction at 8.22, 7.53, and 6.83 mm for the proximal pole, waist, and distal pole respectively. The angle of the male axis existed at an angle of 34.71 degrees from the proximal point directed in a volar-radial direction (►**Fig. 5a–c**). The central axis for the female specimens was calculated to exist along a line with the formula $y = -0.6074x + 7.8852$, $R^2 = 1$, at points calculated in a volar-radial direction at 7.278, 6.670, 6.063 mm for the proximal pole, waist, and distal pole respectively. The angle of the female axis existed at an angle of 31.27 degrees from the

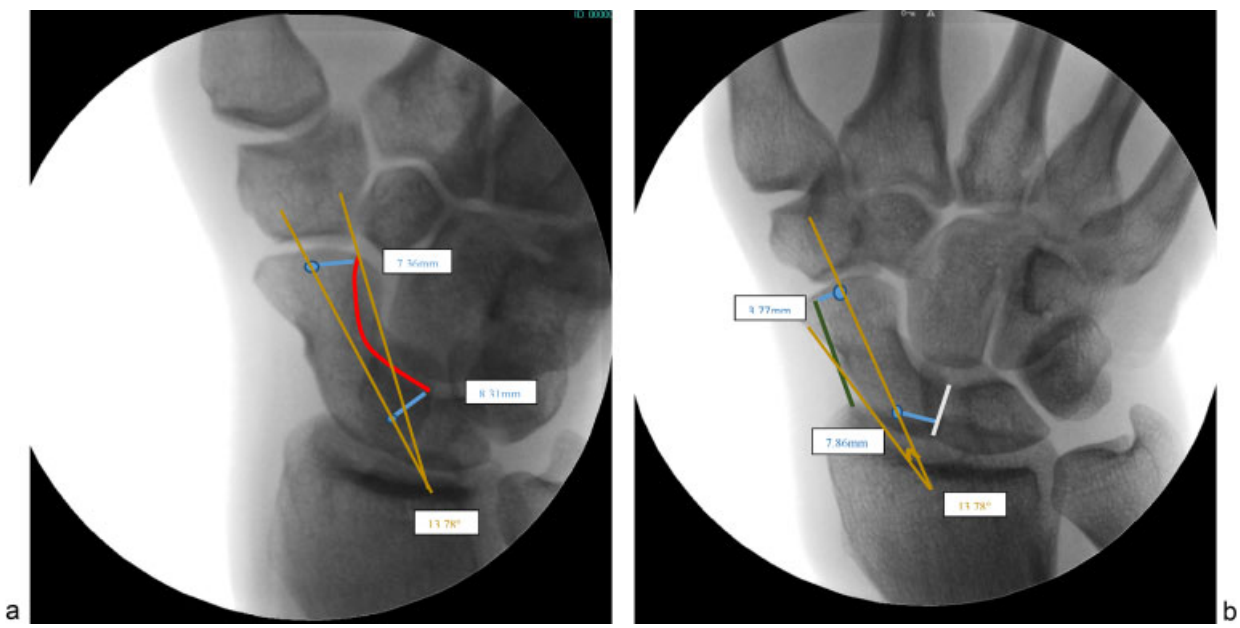

Fig. 3 To-scale interpretation of the position of the central axis of the scaphoid in relation to the scapholunate ligament, the volar radial corner, and the most dorsal point. **(a)** Dorsal-to-volar axis. **(b)** Radioulnar axis. The angle of the axis is represented in gold. The points of the central axis are represented in blue, the dorsal line of the scaphoid is represented in red, the volar radial corner is represented in green, and the scapholunate ligament is represented in gray.

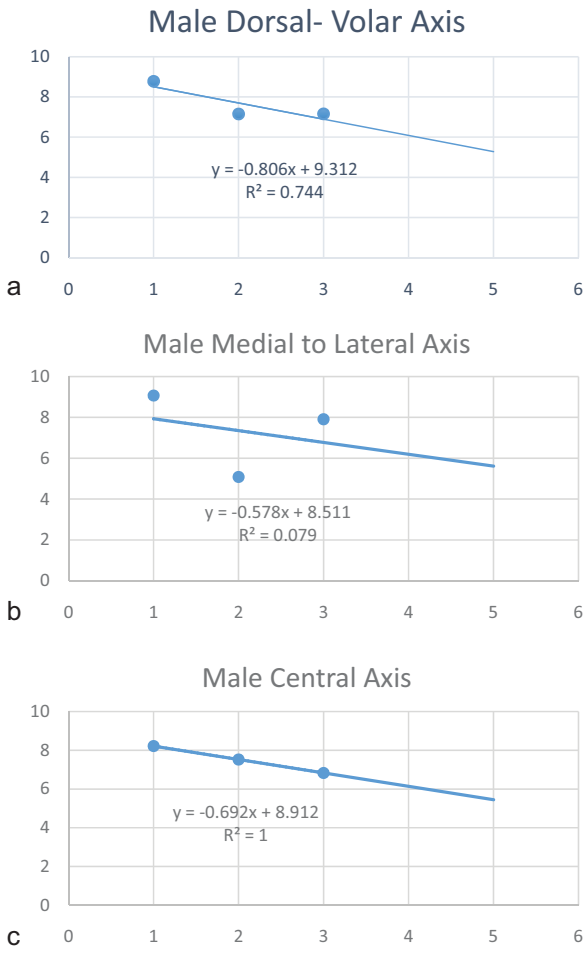

Fig. 4 Scatter plot graphs representing the line of the axes and the overall central axis for the male-specific measurements. The *y*-axis represents a measurement in mm, the *x*-axis represents position from proximal to distal with lower numbers on the *x*-axis representing a proximal position and higher numbers representing a more distal position. **(a)** Dorsal-to-volar axis. **(b)** Medial-to-lateral axis. **(c)** Overall central axis. The equation for the line and the regression analysis value is displayed in each respective plot.

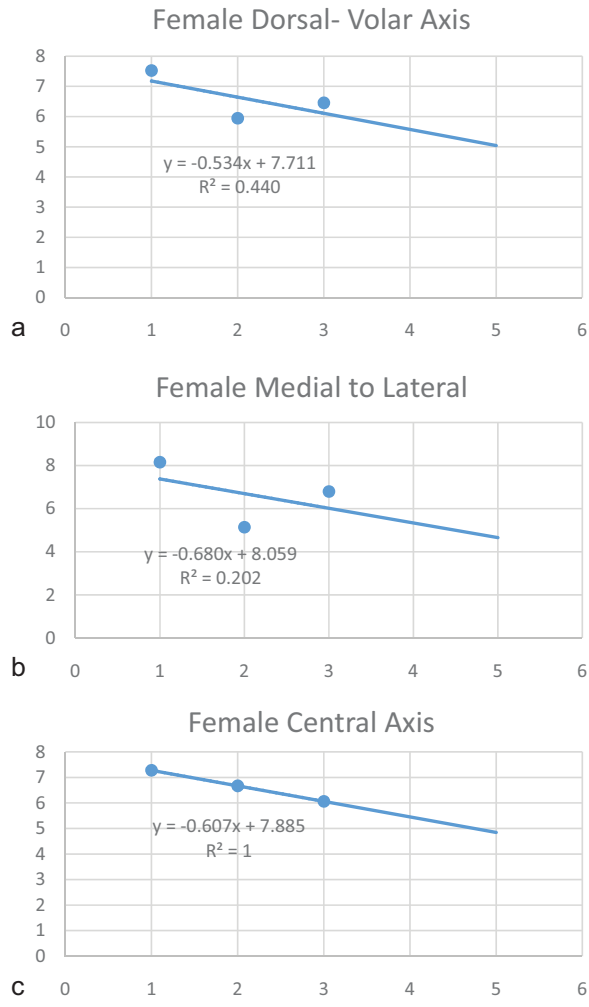

Fig. 5 Scatter plot graphs representing the line of the axes and the overall central axis for the female-specific measurements. The *y*-axis represents a measurement in mm, the *x*-axis represents position from proximal to distal with lower numbers on the *x*-axis representing a proximal position and higher numbers representing a more distal position. **(a)** Represents the dorsal-to-volar axis. **(b)** Represents the medial-to-lateral axis. **(c)** Represents the overall central axis. The equation for the line and the regression analysis value is displayed in each respective plot.

proximal point directed in a volar-radial direction. An unpaired *t*-test was used to compare the male and female measurements and showed no significant difference with a calculated $p = 0.399$.

Discussion

There are multiple techniques described for the treatment of scaphoid fractures. The approach that the treating physician may choose is often based on the class of the fracture defined by Geissler and Slade, as well as the overall stability of the fracture.[2,3,9] Operative fixation is highly recommended for waist and proximal pole fractures, as well as unstable distal pole fractures.[2–5,8] A biomechanical study by McCallister showed an improved prognosis when a cannulated headless screw was placed along the central axis of the scaphoid. The central axis was defined to be the center of the proximal fragment of the fracture. They compared central placement to eccentric, or oblique, screw placement and came to the stated conclusion.[4] Hart et al found that placement of a screw in the central axis of a scaphoid fracture allowed more surface area for fixation, which could correlate to reduced incidence of malunion or nonunion due to decreased compromise of vascularity and increased stability of fixation.[5] With the central axis reproducibly defined by this study, more controlled biomechanical and in vivo studies could occur. This would allow for further elucidation of a true decrease in the incidence of malunion and nonunion, therefore building upon the findings of these studies.

Female scaphoids were overall smaller than the male specimens; however, no significant difference was found between the two cohorts, but the comparison was not done using the true long axis of the wrist and forearm.[8] This finding disagrees with some, and agrees with other previous comparisons of scaphoid measurements between sexes.[6,11–13]

Because there was no significant difference between sexes in this study, it was not necessary to perform separate analyses to define the central axis. The central axis therefore would not require significant adjustments based on patient sex or body morphology.

The central axis of the scaphoid can be described to exist along a line extending from a point on the proximal pole, 7.86 mm radial from the scapholunate ligament and 8.31 mm volar of the most dorsal point; through the waist; and extending to the relative central point of the distal pole measured 3.77 mm ulnar of the volar radial corner and 7.36 mm volar of the most dorsal point. These results place the starting point on the proximal pole more radial than previously described. This more radial position of the proximal starting point may affect the screw length achieved intraoperatively. However, this study may enable the practicing surgeon to ascertain the central axis of the scaphoid more easily based on measurements of the scaphoid, as well as its relationship to surrounding anatomic landmarks; a more radial starting point may not affect the stability of fixation or significantly affect the length of the screw. This study cannot comment on the longest screw length that could be achieved using the previously described measurements. Significant screw length variability was demonstrated by Levitz and Ring, concluding that reliance on intraoperative length measurements was the most accurate determination of screw length.[7]

The present study was able to describe the central axis of the scaphoid with a focus on the dorsal approach; however, the volar approach has been described to be more desirable on the grounds that that increased screw length can theoretically be achieved.[6] The central axis, however, is difficult to achieve using this approach because of the position of the trapezium.[7] Further research would be necessary to determine the axis in a volar approach, as well as the longest screw length that could be achieved.

The use of a handheld measuring device has been shown to be inaccurate. The use of more advanced 3D imaging has been shown to be more accurate when used for measurements on cadaveric specimens, but this accuracy was not shown to be reproducible on living models.[14,15] Assessment of multiple geometric characteristics of the scaphoid performed during this study enabled more accurate measurements with the use of a handheld device; these findings may enable reproduction of these measurements clinically, or intraoperatively with more ease. The description of the central axis in relation to surrounding anatomic landmarks also allows for further ease of reproducibility. However, the results elucidated in this study and their reproducibility in the living model would require further research.

Conflict of Interest
None

References

1 Buijze GA, Lozano-Calderon SA, Strackee SD, Blankevoort L, Jupiter JB. Osseous and ligamentous scaphoid anatomy: Part I. A systematic literature review highlighting controversies. J Hand Surg Am 2011;36(12):1926–1935
2 Buijze GA, Doornberg JN, Ham JS, Ring D, Bhandari M, Poolman RW. Surgical compared with conservative treatment for acute nondisplaced or minimally displaced scaphoid fractures: a systematic review and meta-analysis of randomized controlled trials. J Bone Joint Surg Am 2010;92(6):1534–1544
3 Geissler WB, Adams JE, Bindra RR, Lanzinger WD, Slutsky DJ. Scaphoid fractures: what's hot, what's not. J Bone Joint Surg Am 2012;94(2):169–181
4 McCallister WV, Knight J, Kaliappan R, Trumble TE. Central placement of the screw in simulated fractures of the scaphoid waist: a biomechanical study. J Bone Joint Surg Am 2003;85-A(1):72–77
5 Hart A, Mansuri A, Harvey EJ, Martineau PA. Central versus eccentric internal fixation of acute scaphoid fractures. J Hand Surg Am 2013;38(1):66–71
6 Meermans G, Verstreken F. Influence of screw design, sex, and approach in scaphoid fracture fixation. Clin Orthop Relat Res 2012;470(6):1673–1681
7 Levitz S, Ring D. Retrograde (volar) scaphoid screw insertion—a quantitative computed tomographic analysis. J Hand Surg Am 2005;30(3):543–548
8 Menapace KA, Larabee L, Arnoczky SP, Neginhal VS, Dass AG, Ross LM. Anatomic placement of the Herbert-Whipple screw in scaphoid fractures: a cadaver study. J Hand Surg Am 2001;26(5):883–892
9 Sendher R, Ladd AL. The scaphoid. Orthop Clin North Am 2013;44(1):107–120
10 Dyankova S. Anthropometric characteristics of wrists joint surfaces depending on lunate types. Surg Radiol Anat 2007;29(7):551–559
11 Feipel V, Rinnen D, Rooze M. Postero-anterior radiography of the wrist. Normal database of carpal measurements. Surg Radiol Anat 1998;20(3):221–226
12 Heinzelmann AD, Archer G, Bindra RR. Anthropometry of the human scaphoid. J Hand Surg Am 2007;32(7):1005–1008
13 Pichler W, Windisch G, Schaffler G, Heidari N, Dorr K, Grechenig W. Computer-assisted 3-dimensional anthropometry of the scaphoid. Orthopedics 2010;33(2):85–88
14 Fukuda S, Ishida O, Kido M, Suzumura F, Ikuta Y. A morphological study of the scaphoid using a mathematical technique and comparative study of the three-dimensional measurements of the scaphoid. Hand Surg 2003;8(2):157–161
15 Smith DK. Anatomic features of the carpal scaphoid: validation of biometric measurements and symmetry with three-dimensional MR imaging. Radiology 1993;187(1):187–191